

TEMPORAL EVOLUTION OF INTERMETALLIC DIFFUSE BAND  
SPECTRA

IRENA LABAZAN, DAVORKA AZINOVIĆ, SREĆKO GOGIĆ and SLOBODAN  
MILOŠEVIĆ

*Institute of Physics, P.O.Box 304, HR-10000 Zagreb, Croatia*

Received 10 December 1999; Accepted 24 May 1999

LiZn and LiCd vapour mixtures prepared in the heat-pipe oven are irradiated with pulsed excimer laser emission at 308 nm. Temporal evolution of the fluorescence spectra is observed showing that different processes occur such as multiphoton excitation, collisional energy transfer, photochemical reaction, relaxation etc. Temporal change of the LiZn and LiCd blue-green diffuse bands spectral shape is observed and interpreted in terms of previous spectral simulations. The effective lifetimes of different spectral features are determined.

PACS numbers: 33.10.-n, 33.20.Kf, 33.80.Gj

UDC 539.194, 539.196

Keywords: LiZn – LiCd vapour mixtures, pulsed excimer laser irradiation, temporal evolution of fluorescence spectra, multiphoton excitation, collisional energy transfer, photochemical reaction, relaxation, effective lifetimes

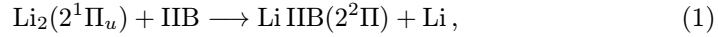
## 1. Introduction

Spectra from intermetallic vapour mixtures are usually quite complicated due to the overlap of different spectral features [1]. A general remedy to this problem is a careful preparation of the alloy composition [2–4]. LiZn and LiCd diffuse band spectra were first reported in Refs. 5 and 6. These experiments were performed with the pulsed laser but only time-averaged spectra were recorded. Subsequent detailed spectral simulations have shown complex nature of the diffuse band spectra [7]. Both bound-bound and bound-free types of transitions were found to play an important role.

When pulsed lasers are used for excitation, different spectral features can be distinguished by performing temporal analysis of spectra with nanosecond resolution [8]. The temporal analysis of alkali-IIB excimer bands was used in the case of

NaCd and NaHg to identify molecular formation channel and relevant rate coefficients [9,10].

In this work we have studied temporal evolution of intermetallic diffuse bands, particularly of the LiZn and LiCd systems produced photochemically in the reaction:



where IIB is Zn or Cd atom. Under conditions of dense vapour mixtures reaction (1) is followed by the thermalization of the nascent population distribution of the  $2^2\Pi$  state



which is responsible for the change in the diffuse bands spectral shapes.

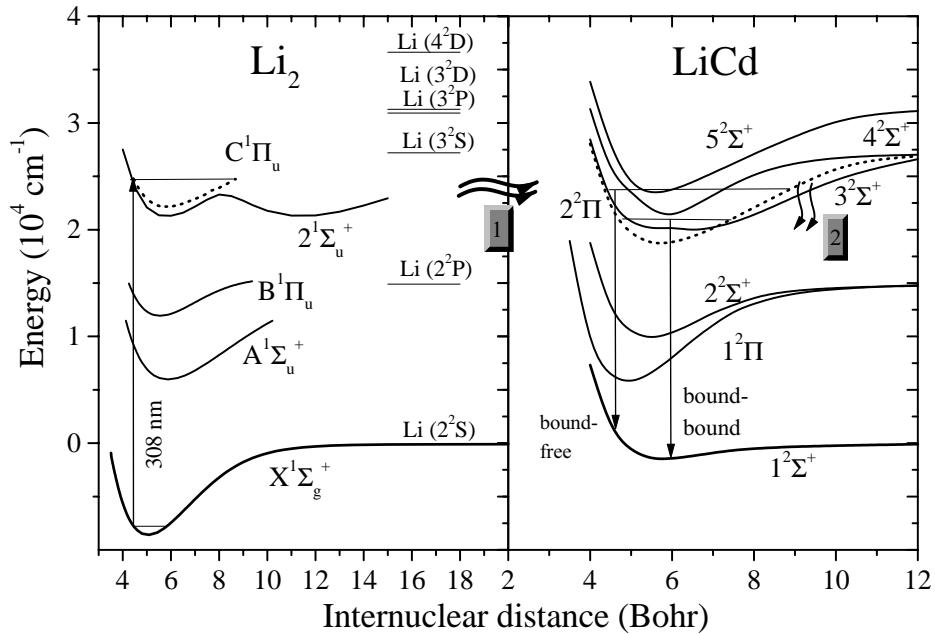


Fig. 1. Partial potential energy diagram of  $\text{Li}_2$  and  $\text{LiCd}$  molecules showing 308 nm excitation, photochemical reaction path, relaxation process and  $\text{LiCd}$  bound-free and bound-bound type of emission.

We use excimer laser at 308 nm to excite  $\text{Li}_2(\text{C}^1\Pi_u)$  and temporal analysis of different spectral features to clarify excitation processes and photochemical production of  $\text{LiZn}$  and  $\text{LiCd}$  molecules. Illustration of the processes (1) and (2) is shown in Fig. 1 for the  $\text{LiCd}$  case.

## 2. Experiment

The experimental arrangement was similar to that described in our previous paper [8]. Metal vapour mixtures were generated in a heat-pipe ovens. The heat-pipe ovens were filled with approximately same amounts of lithium and zinc or cadmium. The temperature in the central region of the heat-pipe oven was varied from 1020 K to 1220 K. Helium or argon were used as buffer gases at pressures from 0.67 to 13.3 kPa (5 to 100) Torr. The heat-pipe mode of operation is established for zinc or cadmium vapour. The preparation of electronically excited  $\text{Li}_2$  molecules in specific rovibrational levels of the  $2(\text{C})^1\Pi_u$  state is achieved by means of the 20 ns pulsed XeCl excimer laser lines at 308 nm (LPX 105E). Laser beam (initially of shape 2x1 cm) was spatially filtered and made parallel with a quartz telescope, having the diameter of 2-3 mm in the center of the heat-pipe oven. The horizontal laser induced fluorescence image was rotated by a Dove prism and focused to the vertical entrance slit of the monochromator. The resolution of the system was of about 0.1 nm. The signal from the photomultiplier with S20 cathode was averaged by means of a box-car averager (Stanford SR245). The analog output from the box-car was converted to digital signal through an A/D converter and fed to a laboratory computer. Temporal analysis is performed by means of a box-car averager or a 8-bit, 150 MHz digital storage oscilloscope (Hameg 1507). Spectral response of our detection system was measured by using a standard calibrated tungsten lamp and is found flat in the region of interest (450-550 nm).

We performed two types of measurements. To measure laser induced fluorescence we scan the monochromator in wavelength interval of interest, setting a specific gate and time delay value of the box-car averager. Time resolved intensity of the fluorescence is measured at a given setting of the monochromator by using a digital storage oscilloscope or by scanning the time delay of a box-car gate. Zero of the time scale is set to the rising edge of the laser pulse.

## 3. Results and discussion

### 3.1. Excitation of Li-Zn vapour mixture

Figure 2 shows the fluorescence of the LiZn vapour mixture in the region from 420 to 500 nm, excited by the laser lines at 308 nm. For short time delay of 10 ns (Fig. 2a) we observed only the LiZn excimer band ( $2^2\Pi - 1^2\Sigma$  transition), peaked at 477 nm [5]. At the delay of 40 ns we noticed Zn atomic lines at 472.2 and 481.2 nm (Fig. 2b) ( $5^3S_1 - 4^3P_1$  and  $5^3S_1 - 4^3P_2$  transitions). For the delay of 70 ns (Fig. 2c) Zn lines decreased substantially. This time behaviour suggests that Zn atoms are populated in near resonant two-photon absorption process  $\text{Zn}(4^1S_0) + 2h\nu + \text{M} \rightarrow \text{Zn}(6^3S_1) + \text{M}$ , where M is Zn or Li atom, followed by a quick cascade emission  $\text{Zn}(6^3S_1) \rightarrow \text{Zn}(5^3P_1) \rightarrow \text{Zn}(5^3S_1)$ . Proposed excitation mechanism of zinc atomic emission is illustrated in Fig. 3. Alternative excitation mechanism which involves energy pooling collision  $4p\ ^3P_J + 4p\ ^3P_J$  can be excluded on the basis of temporal evolution [12]. Energy pooling excitation results with microsecond decay times. As zinc atomic features decrease, Li atomic lines

at 460.3 and 497.2 nm appear (4D-2P and 4S-2P transitions) in spectra. Lithium atomic spectral features are consequence of the dissociative recombination of  $\text{Li}_2^+$ , the latter being produced via  $\text{Li}_2(\text{C}^1\Pi_u) + h\nu \rightarrow \text{Li}_2^+ + e$  process.

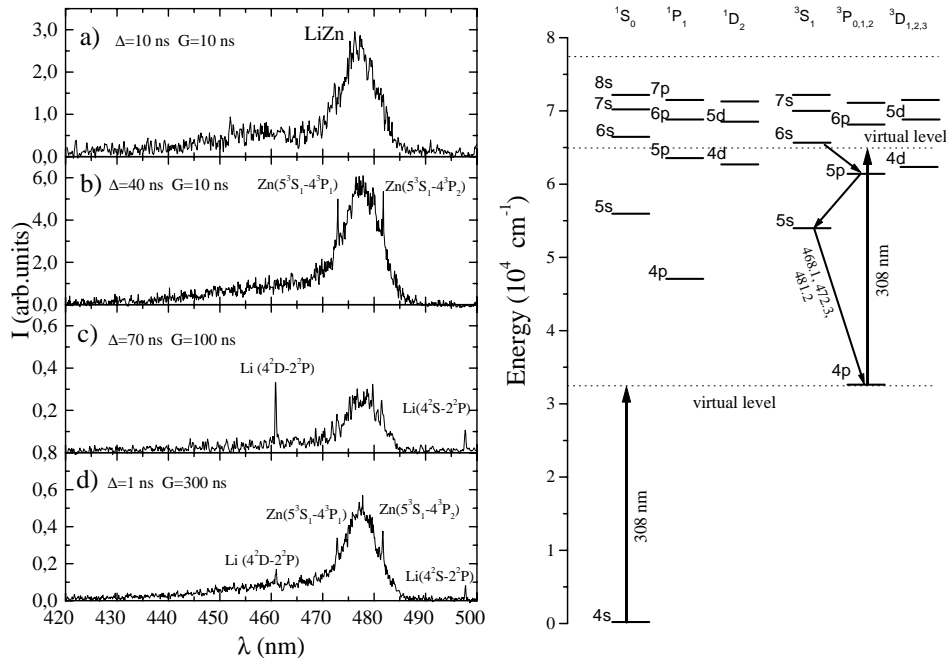


Fig. 2. The spectra of the Li-Zn vapour mixture excited by 308 nm laser lines at Ar pressure of 6.9 kPa (52 Torr) and temperature  $T = 1050$  K. Time delays and gates are: a)  $\Delta = 10$  ns,  $G = 10$  ns, b)  $\Delta = 40$  ns,  $G = 10$  ns, c)  $\Delta = 70$  ns,  $G = 100$  ns and d)  $\Delta = 1$  ns,  $G = 300$  ns.

Fig. 3 (right). Term diagram of zinc atom illustrating excitation mechanism of a high-lying levels by 308 nm photons. Data are taken from Ref. 11. The energy defect for the first step is about  $30 \text{ cm}^{-1}$  and for the second step  $490 \text{ cm}^{-1}$ .

Figure 2d shows spectrum with large gate of the box-car averager which should be compared with the time averaged spectra (see Ref. 5). Following the sequence from a to c, we observe change of the LiZn band shape. The band tail extending from 470 nm to 440 nm, visible also in the time-averaged spectrum (Fig. 2d), is most pronounced for earliest time delays. The ratio of intensities at band maximum (477 nm) and band tail (455 nm) changes from 1/4, 1/7 to 1/14. According to spectral simulations presented in Ref. 7 this long tail is of bound-free nature and originates from higher vibrational states of the  $2^2\Pi$  state ( $v' \geq 7$ ). Therefore, the observed change in the band shape indicates relaxation of the nascent population distribution which is obviously centered at high rovibrational levels of the  $2^2\Pi$  state.

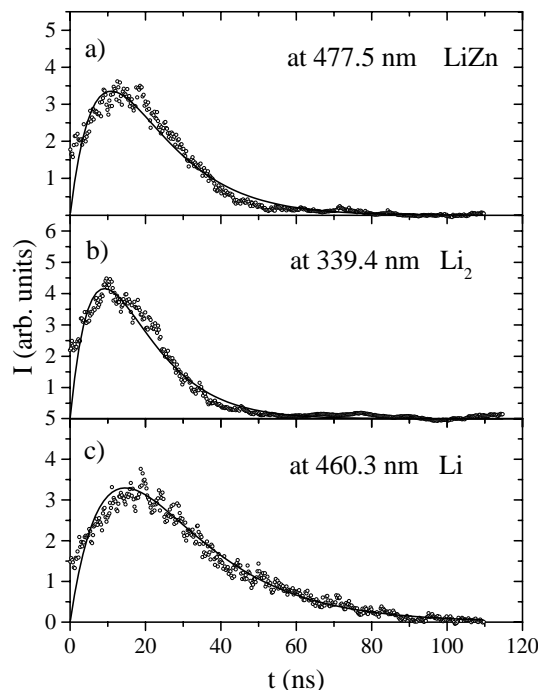


Fig. 4. Temporal evolution at a) LiZn band (477.5 nm), b)  $\text{Li}_2\text{C}^1\Pi_u\text{-X}^1\Sigma_g^+$  band (339.4 nm), and c)  $\text{Li}4^2\text{D-}2^2\text{P}$  atomic line (460.3 nm). Temperature was  $T = 1050$  K and argon buffer gas pressure 8.4 kPa (11 Torr). The full curve represents a double-exponential fit of the experimental values.

The temporal evolutions at a) 477.5 nm (LiZn), b) 339.4 nm ( $\text{Li}_2$  C state) and c) 460.3 nm (Li) are shown in Fig. 4. We have determined the effective lifetimes of the corresponding emissions, which are at  $T = 1050$  K and  $(12 \pm 5)$  ns for  $\text{LiZn}(2^2\Pi)$ ,  $(10 \pm 3)$  ns for  $\text{Li}_2(2^1\Pi_u)$  and  $(19 \pm 3)$  ns for  $\text{Li}(4^2\text{D})$  state. With increasing temperature the metal vapour pressure increases causing the  $\text{LiZn}(2^2\Pi)$  effective lifetime to decrease linearly, i.e. at 990 K  $\tau_{eff} = (20 \pm 5)$  ns and at 1060 K  $\tau_{eff} = (8.5 \pm 4)$  ns. The lifetime is approximated by the extrapolation to the zeroth zinc vapour pressure at 723 K, which gives  $\tau_{rad} = (65 \pm 26)$  ns.

### 3.2. Excitation of Li-Cd vapour mixture

Figure 5 shows spectra of the Li-Cd vapour mixture excited by 308 nm laser lines at  $T = 1030$  K and a)  $\Delta = 25$  ns and  $G = 10$  ns, b)  $\Delta = 50$  ns and  $G = 10$  ns, c)  $\Delta = 70$  ns and  $G = 75$  ns and d) time-averaged  $\Delta = 10$  ns and  $G = 200$  ns. Excited  $\text{LiCd}(2^2\Pi)$  molecules are produced through the photochemical reaction [7] with nascent rovibrational population distribution far from Boltzmann distribution (see Fig. 1), which gives dominant bound-free emission for short time delays

after the laser pulse (Fig. 5a). Subsequent collisions with Cd atoms are efficiently thermalizing the nascent rovibrational population. This is observed, for larger time delays (see Fig. 5b and 5c), as the change of spectral shape of the blue-green diffuse band, with dominant bound-bound contribution to the emission [7] (sharp peaks near the band maxima). In the present experiment we do not observe cadmium atomic lines in the spectral region shown in Fig. 5, neither the characteristic emission at 326.1 nm ( $5p\ ^3P_1 - 5s\ ^1S_0$  transition). The latter was observed in Ref. 13 for Cd-He mixtures where 308 nm excitation was explained to proceed through the characteristic features of the Cd-He collision complex. Although one could expect rather similar structure of the Cd-He and Cd-Ar or Cd-Li complexes they are quite different in respect to the efficiency of specific collisional energy transfer process. This shows that careful preparation of metal mixtures and choice of a buffer gas can be used to efficiently promote different spectral features. Lithium atomic lines appear after 70 ns similarly as in the LiZn case. We note that, as in LiZn case,

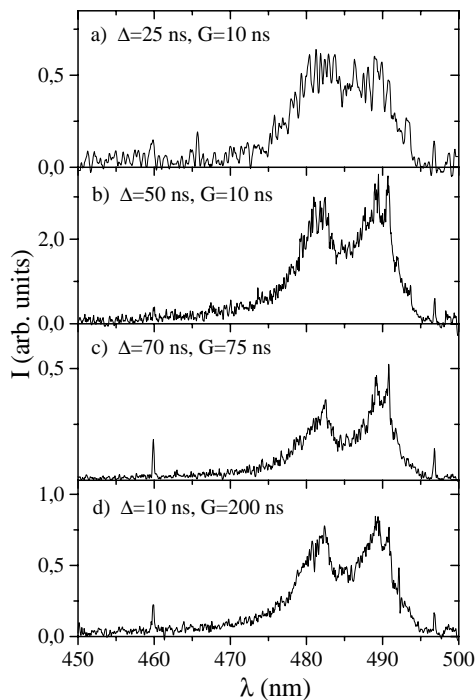


Fig. 5. The spectra of the Li-Cd vapour mixture excited by 308 nm laser lines at Ar pressure of 13 kPa (100 Torr) and temperature  $T = 1030$  K for different sets [(a) to (d)] of time delay and gate.

$\text{Li}_2$  spectral features (diffuse band at 458 nm) are absent from spectra. This is an indication of the low Li and  $\text{Li}_2$  density in the vapour mixture above liquid alloy.

Figure 6 shows LiCd diffuse band spectra in the region 450 - 500 nm recorded at

the time delay of 75 ns for different buffer gas (Ar) pressures. We assume that for all cases the heat-pipe works in the heat-pipe mode for cadmium, namely central heated part mainly contains cadmium vapours with small portion of lithium vapour (few percent), while buffer gas fill space between heated zone and windows of the heat pipe. Therefore the change of the diffuse band shape is caused by collisions given by process of type (2). For a low buffer gas pressures the diffuse band shape preserve bound-free nature even at large time delays.

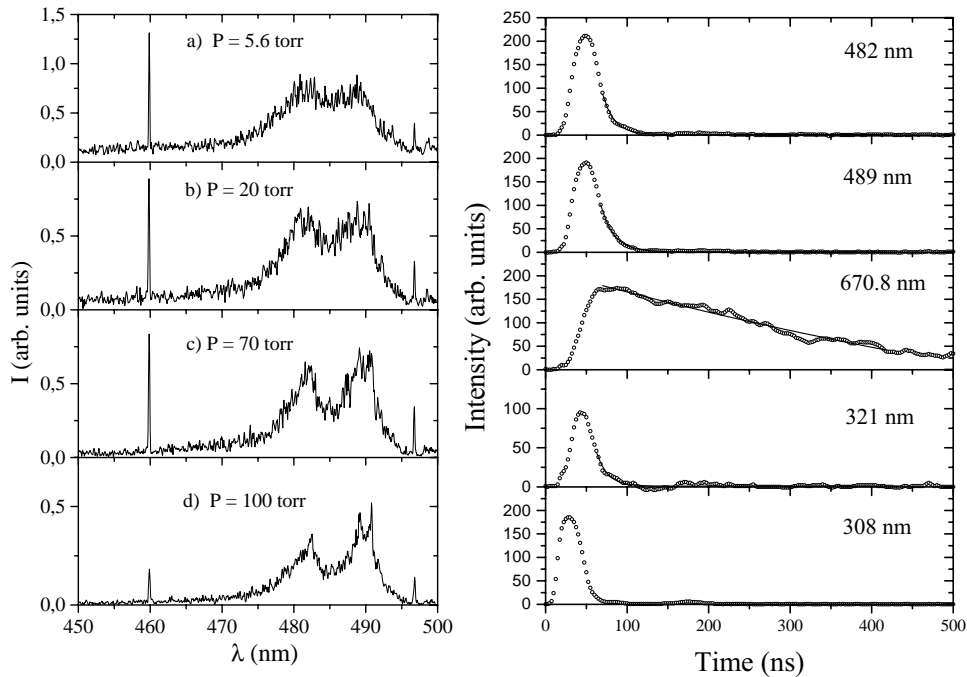


Fig. 6. The spectra of the Li-Cd vapour mixture excited by 308 nm laser taken with time delay  $\Delta = 75$  ns and gate  $G = 60$  ns for different buffer (Ar) gas pressures.  $T = 1000$  K.

Fig. 7 (right). Temporal evolution of different spectral features from LiCd vapour mixture irradiated by 308 nm laser. From the top to bottom fluorescence is shown for: two LiCd diffuse band maxima, 2P-2S lithium transition, Stokes emission within C-X manifold and scattered light of the laser pulse. Temperature was 1040 K and buffer gas pressure 7.4 kPa (5.6 Torr).

Figure 7 shows the time evolution of different spectral features obtained by means of a digital oscilloscope. Set of such curves have been measured for different buffer gas pressures. From each curve decay times were determined by performing single-exponential fit starting at about 60 ns (falling edge of the laser pulse). This is

done in order to avoid influence of the laser pulse width. Plotting effective radiation rates (inverse of decay time) versus Cd atom density allows us to determine the total quenching rate coefficients for relevant upper levels (see Fig. 8). Data for zero cadmium density are obtained from measurement in the pure lithium heat-pipe oven at the same temperature and buffer gas pressure. We note that emission from 2P level is strongly influenced by radiation trapping. We obtain quenching rate coefficient for the Li(2P) level to be  $(3 \pm 1) \cdot 10^{-12} \text{ cm}^3 \text{ s}^{-1}$  and for the C  $^1\Pi_u$  ( $v' \approx 13-19$ ) Li<sub>2</sub> levels  $(1.2 \pm 0.5) \cdot 10^{-11} \text{ cm}^3 \text{ s}^{-1}$ . The effective lifetimes of LiCd spectral features at 489 nm and 482 nm were determined to be 15 ns and 14 ns, respectively. We did not observe significant change of the effective lifetimes with atom density as in the LiZn case.

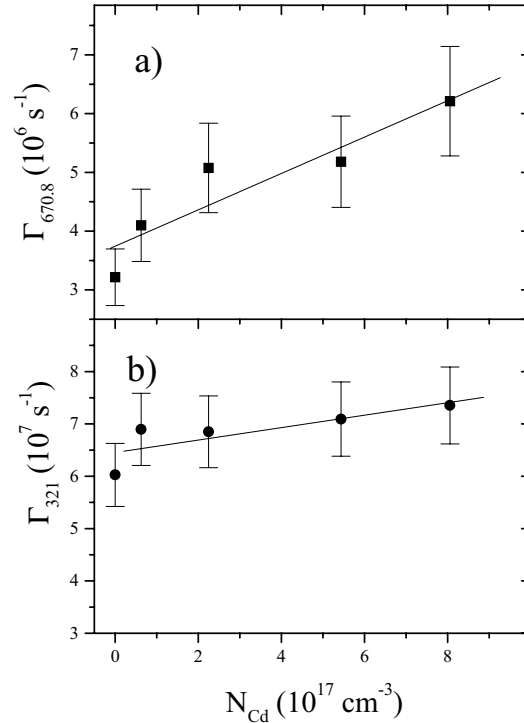


Fig. 8. The effective radiative rates of a) Li(2P) and b) Li<sub>2</sub>(C-X) band versus cadmium atom density for  $T = 1040$  K. The natural radiative rate of Li(2P) is  $3.69 \cdot 10^7 \text{ s}^{-1}$  [14]. The natural radiative rate of the C-state is about  $1.6 \cdot 10^7 \text{ s}^{-1}$  [15].

#### 4. Conclusions

We have shown that, in spite of the relatively large collision frequencies for total pressures usually used within the heat-pipe ovens, nanosecond time spectral analy-

ses can provide important information for understanding of complicated processes in intermetallic vapour mixtures. Photochemical production of the LiZn( $2^2\Pi$ ) and LiCd( $2^2\Pi$ ) excimers by means of 308 nm laser photons results with population of high vibrational states. By performing temporal spectral analysis we observed the redistribution of the population towards the lower vibrational states which completes after the time delays larger than 50 ns. The observed changes in the diffuse band shapes are consistent with predictions of detailed spectral simulations given in Ref. 7. The thermalization effect is especially pronounced in the case of LiCd through appearance of bound-bound structures, which originate from lower vibrational levels in the upper state. Measured effective lifetimes of the LiZn and LiCd emission are similar as those reported for NaCd and NaHg excimers [9,10].

#### Acknowledgements

This work was financially supported by the Ministry of Science and Technology of the Republic of Croatia. We wish to thank Dr. Goran Pichler for valuable discussions and continuous support of this work.

#### References

- 1) S. Milošević, in *Spectral Line Shapes*, Vol. 8, Eds. A. D. May, J. R. Drummond and E. Oks, AIP Conf. Proc. 328 (1995) pp. 391-405.
- 2) D. Azinović, X. Li, S. Milošević, G. Pichler, M. C. van Hemert and R. Düren, *J. Chem. Phys.* **98** (1993) 4672;
- 3) D. Azinović, S. Milošević and G. Pichler, *Chem. Phys. Lett.* **233** (1995) 477;
- 4) D. Azinović, S. Milošević and G. Pichler, *Z. Physik D* **36** (1996) 147;
- 5) S. Milošević, X. Li, D. Azinović, G. Pichler, M. C. van Hemert, A. Stehouwer and R. Düren, *J. Chem. Phys.* **96** (1992) 7364;
- 6) M. C. van Hemert, D. Azinović, X. Li, S. Milošević, G. Pichler and R. Düren, *Chem. Phys. Lett.* **200** (1992) 97;
- 7) X. Li, S. Milošević, D. Azinović, G. Pichler, R. Düren and M. C. van Hemert, *Z. Phys. D* **30** (1994) 39;
- 8) D. Azinović, S. Milošević and G. Pichler, *Fizika A* **5** (1996) 167;
- 9) D. Gruber, U. Domiaty, L. Windholtz, H. Jeager, M. Muso, M. Allegrini, F. Fuso and A. Winkler, *J. Chem. Phys.* **100** (1994) 8103;
- 10) D. Gruber, U. Domiaty, K. Iskra, S. Dinev and L. Windholz, *J. Phys. Chem.* **100** (1996) 7078;
- 11) C. E. Moore, *Atomic Energy Levels*, Vol. II, NBS 467 (1952) p. 124;
- 12) H. Umemoto, A. Masaki, J. Kikuma and S. Sato, *Chem. Phys.* **141** (1990) 457;
- 13) H. Umemoto, T. Ohnuma and A. Masaki, *Chem. Phys. Lett.* **171** (1990) 357;
- 14) W. I. McAlexander, E. R. I. Abraham and R. G. Hulet, *Phys. Rev. A* **54** (1996) R5;
- 15) Th. Weyh, K. Ahmed and W. Demtröder, *Chem. Phys. Lett.* **248** (1996) 442.

## VREMENSKI RAZVOJ INTERMETALNIH DIFUZNIH SPEKTARA

Mješavine para Li-Zn i Li-Cd pripremili smo u toplovodnim pećima i obasjavali pulsnim excimerskim laserom na 308 nm. Opažanje vremenskog razvoja fluorescentnih spektara pokazalo je postojanje različitih procesa kao što je multifotonska pobuda, sudarni prijenos energije, fotokemijska reakcija, relaksacija itd. Opaženu vremensku promjenu spektralnog oblika plavo-zelenih difuznih vrpca LiZn i LiCd molekula objasnili smo pomoću ranijih svojstava spektralnih simulacija. Odredili smo efektivna vremena života različitih spektralnih pojava.